1 Results from Prior NSF Support

Our research group has enjoyed prior support from the National Science Foundation through the recent project "Multiwavelength Observations & Numerical Simulations of Galaxy Cluster Evolution" (award number 9896039 from September 1st, 1997 through April 30th, 1999). The total amount of funding was $130,000 and this was a continuing grant. This project studied clusters of galaxies in the optical, radio and X-ray with an additional emphasis on numerical simulations to guide the interpretation of the observations.

Reviews of this research, at the intersection of observations and theory, are given in Burns (1998) and Burns et al. (2002). On the observational side, a study of the X-ray and optical properties of 25 radio galaxies (not identified as members of Abell clusters) in the nearby Universe ($z < 0.06$) found that FR-I radio sources tend to be found in cluster environments with extended X-ray emission while none of the FR-II radio galaxies were associated with extended emission (Miller et al. 1999). In a study of 22 intermediate redshift ($z \sim 0.2$), X-ray bright clusters, Rizza et al. (2003) found that high luminosity radio galaxies (primarily AGN) reside in galaxies with old stellar populations and that the galaxies are centrally condensed. Conversely, they found that low luminosity radio galaxies (dominated by star bursts), had a range of stellar ages and were more uniformly distributed in the clusters. The radio galaxy fraction did not show a correlation with the cluster's blue galaxy fraction but shows an anticorrelation with cluster richness. Pinkney et al. (2000) doubled the number of Abell clusters containing wide-angled tailed (WAT) radio sources with more than 10 redshifts for cluster member galaxies (18 clusters total), enabling a study of substructure within these clusters. Ledlow et al. (1999) measured the local X-ray luminosity function (XLF) for 294 Abell clusters in the *ROSAT* All Sky Survey (RASS) and found that adiabatic physics alone could not match the XLF but modifications in the mass luminosity relation yielded a best fit for a low density Universe ($\Omega_m < 0.4$). Statistical studies of the cluster environment demonstrated both that classical cooling flow clusters tend to reside in denser environments (Loken et al. 1999) while Novikov et al. (1999) found that the bisector angle of WATs aligns with the axes of the supercluster environment. Finally, this project saw the completion and publication of the WBL catalog of poor galaxy clusters, containing 732 optically identified clusters (White et al. 1999).

Numerical simulations of mergers between idealized clusters were performed to map out the range of cooling flow strengths and other cluster parameters that favor disruption (Gómez et al. 2002), finding the ram pressure of the infalling cluster was of primary importance but the post-merger cooling time could still be short compared to the Hubble time. Kurt Roettiger applied MHD simulations of merging clusters to both study the amplification of magnetic fields to power radio halos (Roettiger et al. 1999a) and investigate Abell 3667; showing that the extended radio emission was consistent with predictions for a recent, off-axis merger (Roettiger et al. 1999b). In a study of three cooling flow clusters with strong, core radio sources and excess X-ray emission associated with the radio source region (as seen by *ROSAT*), Rizza et al. (2000) demonstrated through numerical simulations that the AGN jet - interacting with the cluster atmosphere - could produce similar enhancements and decrements in the X-ray surface brightness. These structures, seen with the resolution of *Chandra*, now appear as well defined cavities or bubbles (see Figure 8 for a *Chandra* image of Abell 2052, one of the sample clusters). Finally, data from our first cosmological simulations were examined from the point of view of weak lensing to gauge "projection bias" due to structure along the line of sight but not part of the cluster itself. Metzler et al. (1999) found that weak lensing masses could significantly over-estimate the true mass of the cluster.

2 Introduction

In the current proposal we focus our attention on the application of our detailed, cosmological simulations of clusters of galaxies to the Sunyaev-Zeldovich effect (SZE; Sunyaev & Zeldovich 1970; 1972). We are motivated by the tremendous promise of SZE observations as well as the unique contribution our work can make in the interpretation of these data. Despite the need for brevity in proposals such as this, some review of the basic physics of the SZE is warranted to provide a common framework for the discussion that follows. The SZE is the inverse Compton scattering of photons from the cosmic microwave background (CMB) from higher energy electrons in the atmospheres of clusters of galaxies. The change in intensity of the CMB at a point in the sky due to the SZE can be expressed, using notation similar to the recent review of the SZE by Carlstrom et al. (2002), as

$$\frac{\Delta I_{SZE}}{I_0} = g\left(x\right) y - h\left(x\right) b \tag{1}$$

where x is a dimensionless frequency ($x = h\nu / k_B T_{CMB}$) and $I_0 = 2\left(k_B T_{CMB}\right)^3 / \left(hc\right)^2$. The terms on the right hand side correspond to the thermal and kinetic SZE, respectively, and g and h are (in the non-relativistic limit) dependent solely on the frequency of the observation while y and b depend only on parameters integrated along the line of sight through the cluster. It is important to note that the SZE is a distortion of the CMB. The CMB radiation does suffer cosmological dimming with increasing redshift. However, the **ratio** of the SZE to the CMB does not. Therefore, eq (1) is independent of redshift. Cluster surveys with the SZE have a very different selection function than optical or X-ray surveys, with the ability to find a larger number of distant structures. The Compton y parameter is given by

$$y = \int \frac{k_B T_e}{m_e c^2} n_e \sigma_T dl \tag{2}$$

where k_B is Boltzman's constant, T_e is the temperature of the cluster electrons, $m_e c^2$ is the electron rest mass energy, n_e is the electron number density, σ_T is the Thompson cross section and the integration is performed along the line of sight. The kinetic term is the Doppler shift arising from flows along the line of sight and is given by

$$b = \int n_e \sigma_T \frac{\mathbf{v}}{c} \cdot \mathbf{dl} \tag{3}$$

where $\mathbf{v}$ is the velocity of the gas.

To make connection with observations, we are interested in integrals over some finite solid angle on the sky

$$Y = \int y d\Omega = \frac{1}{d_A^2} \int_A y dA = \frac{k_B \sigma_T}{m_e c^2 d_A^2} \int_V T_e n_e dV \tag{4}$$

where d_A is the angular diameter distance. The integrated thermal SZE signal simply measures the thermal energy content of a cluster. To compare intrinsic cluster properties we also use the distance independent quantity,

$$Y^{int} = Y d_A^2. \tag{5}$$

By examining estimates for a typical cluster of galaxies we can see why observations of the SZE have been so challenging. For an isothermal, 5 keV cluster with $\bar{n}_e \sim 10^{-3}\ cm^{-3}$, the optical depth to Compton scattering is $\sim 10^{-2}$ while the mean relative frequency shift in the CMB photons is approximately $\frac{k_B T_e}{m_e c^2} \sim 10^{-2}$. The thermal SZE then constitutes a mean, relative intensity change of $\sim 10^{-4}$. The kinetic SZE, for a flow velocity of $\sim 1,000\ km\ s^{-1}$, is about a factor of 100 smaller still. Since the first reliable detections of the SZE in the 1970's (e.g. Birkinshaw et al. 1978) observations of the SZE have become somewhat routine despite these challenges and as we shall see, a multitude of observational programs exist.

2.1 Current Observational Efforts

The SZE has, in recent years, been used by many research teams in the United States and around the world to study clusters of galaxies. A comprehensive survey of observations through the late 1990's has been given by Birkinshaw (1999). Instruments for detecting the SZE that are currently in operation or in development include interferometers such as **OVRO**, the **BIMA** array, the **SZA**, (these three instruments will be combined to form **CARMA**), the Ryle telescope array, AMI, **CBI**, AMiBA and **ALMA**.

For reference, instruments funded in part or full by the National Science Foundation are indicated in boldface. Recent progress in bolometer arrays has facilitated a complementary set of instruments based on this technology including **SuZIE**, **ACBAR**, the **Bolocam** project (Jason Glenn, a member of the Bolocam team is also a faculty member at the University of Colorado), APEX-SZ, ACT and the **SPT**. In addition, the Planck mission should discover of order $1,000$ clusters despite its relatively poor angular resolution ($5'$ at best compared to $\sim 1'$ for the other experiments listed above; White 2003). Clearly the astronomical community has invested significant effort to bring the promise of the SZE to fruition.

The SZE is certainly not the only tool available to study clusters. Of particular importance are optical observations that can determine photometric redshifts accurately and rapidly with large format CCD arrays (e.g. Yee & Gladders 2002). With *Hubble* and ground-based facilities, observers have also mapped the total mass distribution in clusters through weak lensing (Kneib et al. 2003; Hoekstra et al. 2002). Supporting, high-resolution data from X-ray satellites such as *Chandra*, *XMM* and *ASTROE-2* are likewise crucial to the success of SZE surveys.

In Table 1 we provide a partial list of applications of SZE observations along with a recent, illustrative reference. SZE clusters observed in blind surveys to measure cosmological parameters are of particular importance and warrant more discussion. These efforts involve measurement of the SZE and redshifts of clusters, converting the observed SZE into a mass and comparing the mass function of the survey clusters to predictions from cosmological models. As outlined in Carlstrom et al. (2002), a deep SZE survey covering 12 square degrees will enable confirming measurements of the density of both matter and dark energy (Ω_m and Ω_Λ) and a 5% measurement of σ_8 (the normalization of fluctuations on a comoving 8 h^{-1} Mpc length scale). The value of σ_8 is currently discrepant between low ($\sigma_8 \sim 0.7$; primarily based on X-ray observations, see Allen et al. 2003; Voevodkin & Vikhlinin 2003) and higher values inferred from observations of the CMB ($\sigma_8 \sim 1$; cf Bond et al. 2002). From the work of Mohr et al. (2002), we see that a hypothetical survey with the South Pole Telescope (SPT) covering 4,000 square degrees will detect $\sim 17,000$ clusters and can measure the dark energy equation of state to $\sim 5\%$ accuracy - *provided that the systematic errors in the mass estimate can be kept to within* $\sim 10\%$.

Extensive effort has been expended to reduce the systematic uncertainties in SZE observations. The difficult problems of flux calibration, source confusion, atmospheric effects and accurate beam descriptions have received considerable attention (see Reese 2003 for an example of this effort for an interferometer). Fundamental theoretical calculations of the SZE effect including relativistic corrections and/or multiple scattering have also gained considerable attention to bring the models closer to reality (Sazonov & Sunyaev 1998; Nozawa et al. 1998; Itoh et al. 1998; Shimon & Rephaeli 2002; Nozawa & Itoh 2003). Furthermore, given the number of SZ instruments, it is manifest that large samples of clusters (of order thousands to tens of thousands) will soon be in hand to greatly reduce the statistical uncertainty in ensemble measurements. While these advances are all requisite and commendable we note one class of effort in great need of increased diligence. *The fundamental "picture" of clusters assumed in the interpretation of SZE data stands in stark contrast to what we and others see in our numerical simulations of structure formation.* Clusters simply are **not** isolated, isothermal, static, spheres of gas.

Of these assumptions, we have previously demonstrated that it is unlikely that clusters are isothermal (Loken et al. 2002 and Figure 2), especially out to the relatively large radii sampled in the thermal SZE. Nor are they spherical or in exact hydrostatic equilibrium (Roettiger et al. 1997). We especially emphasize that clusters are not static. Clusters are dynamically young and interact with the surrounding environment - most spectacularly through mergers that are the most energetic events in the Universe since the Big Bang (Sarazin 2001). Interactions will

Table 1: SZE Applications

Application	Reference
H_0 through combination with X-ray data	Reese et al. (2002)
baryon fraction in clusters	Grego et al. (2001)
measure mass-weighted cluster temperatures from SZE only	Hansen et al. (2002)
map peculiar velocity field through kinetic SZE	Benson et al. (2003)
test ΛCDM	Carlstrom et al. (2002)
study dark energy	Majumdar & Mohr (2003)
probe non-thermal electron populations in clusters	Shimon & Rephaeli (2002)
map epoch(s) of reionization through kinetic SZE	Zhang et al. (2003)
directly detect ensembles of Pop III SNe	Oh et al. (2003)

become only more frequent at higher redshift and this is precisely the regime where supporting data in the X-ray will be, at best, extremely costly with current instruments. Thus, detailed numerical simulations of the SZE are essential to understanding what we see through this new window to the high redshift Universe.

We therefore propose to conduct numerical simulations of cluster formation and evolution using a sophisticated and well-tested cosmology code to aid in the interpretation of cluster observations and help calibrate the systematic uncertainties that arise linking the observables to physical quantities and cosmological parameters. Our simulations, utilizing the *enzo* code (Bryan & Norman 1997; Bryan & Norman 1999; Abel et al. 2002; http://cosmos.ucsd.edu/∼enzo) are noteworthy in several respects. First, we use the powerful technique of adaptive mesh refinement (AMR; Berger & Oliger 1984) to obtain high spatial and temporal resolution within the clusters (our current generation of simulations have a peak resolution of ~ 1 *kpc* but we will increase this to ~ 0.1 *kpc* in some simulations) while simultaneously evolving a cosmological sample of the Universe. Second, our code currently incorporates several advanced physics modules including radiative cooling and star formation with supernova feedback. Since we use an Eulerian, or grid-based approach, we can utilize the powerful and well tested Piecewise Parabolic Method (PPM; Colella & Woodward 1984). The PPM scheme is of particular importance because of its excellent shock capturing properties (through high-order interpolation and a Riemann solver) which are crucial to the accurate treatment of the numerous mergers a typical cluster undergoes.

We also propose to continue our practice of making our simulation data available to the astronomical community through the Simulated Cluster Archive (SCA; http://sca.ncsa.uiuc.edu). The archive interface provides interactive tools to manipulate, analyze and extract data from the simulations. For example, it allows observers to prepare synthetic observations of our clusters as viewed through their X-ray emission (in a user-specified waveband), thermal and kinetic SZEs and construct projected, emission-weighted temperature maps.

2.2 Current Simulation Efforts

Before delving into the details of the proposed research we would like to provide an overview of our progress to date as this will help motivate the significant, though feasible, contribution we can make to the interpretation of clusters viewed through the SZE. From a cosmological volume 256 Mpc on a side and assuming a standard ΛCDM model, we have constructed a sample of approximately 75 clusters in the mass range from 4×10^{14} $M_\odot$ to 2×10^{15} $M_\odot$. This sample has been reproduced in four limiting cases. Our first sample was run with what we term the adiabatic model and is based on the most secure input physics - the infall of baryonic fluid into dark matter potential wells with the associated gravitational and shock heating of the fluid (Loken et al. 2002). This serves as our baseline model

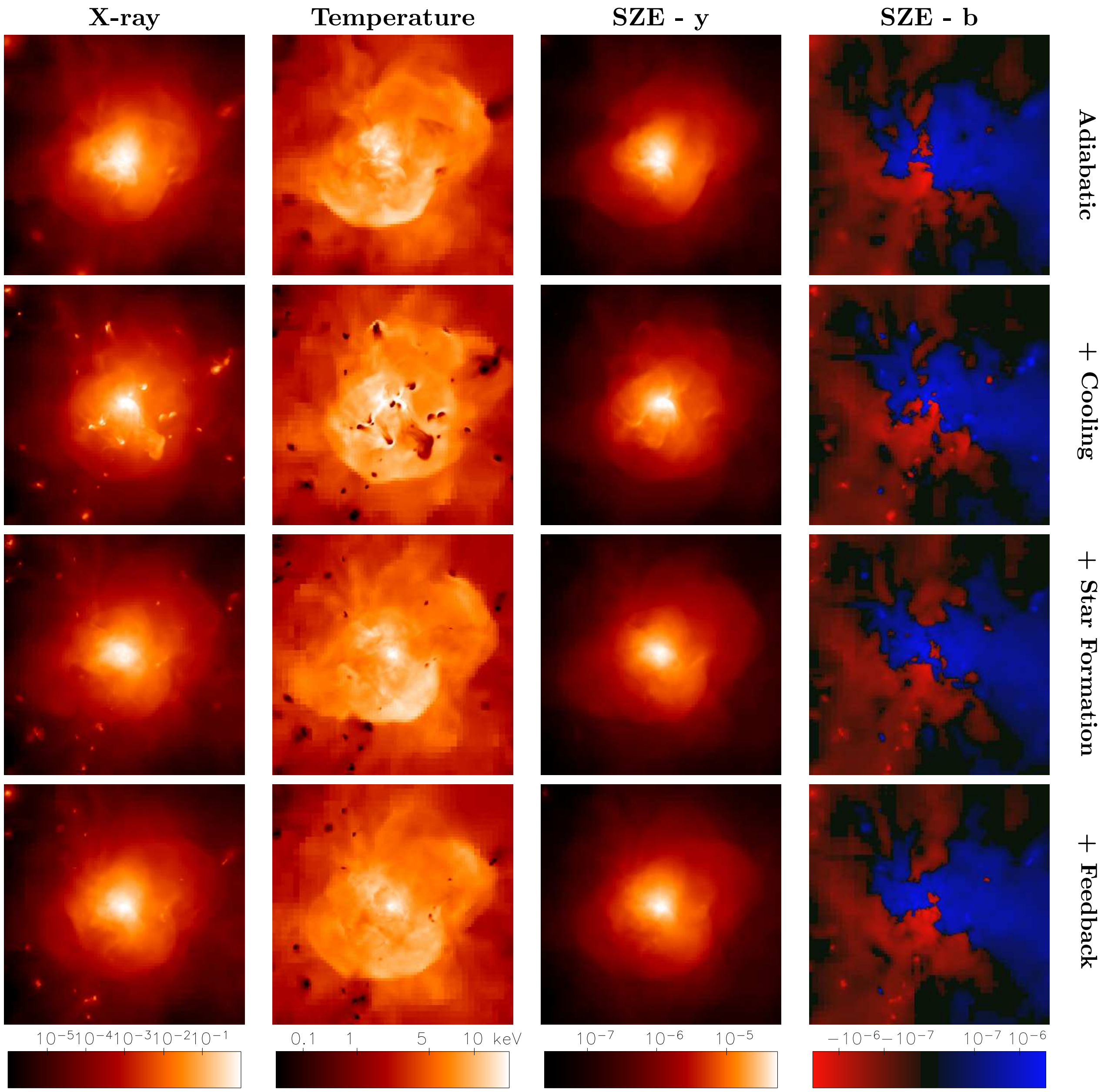

Figure 1: From left to right in each row, we show synthetic (normalized) X-ray images, projected, emission-weighted temperature maps and maps of the projected thermal SZE parameter (y) and kinetic SZE parameter (b) at the present epoch for the same cluster evolved in the indicated physical limit. The simulations were all completed at the same peak spatial resolution of 15.6 kpc and show a field of view 5 Mpc on a side centered on the cluster center of mass. The dynamic range of the images are set by the values in the adiabatic images and are indicated in the colorbars at bottom.

and in detail it tracks the predictions of the self-similar cluster model (Kaiser 1986), a non-trivial test of our basic simulation tool. The next level of complexity we have included is radiative cooling (Burns et al. 2003; Motl et al. 2003a). In each timestep, the fluid loses energy in accord with a tabulated cooling curve derived from a Raymond-Smith emission model for a fixed 0.3 solar metallicity plasma. We note that the cooling curve is truncated at a lower temperature of $\sim 10^5$ K. The cooling model represents the case of as many baryons cooling as possible with no dropout or feedback mechanisms. In other words, it is not feasible to cool more of the fluid than in this limiting case. We have also reproduced our sample with star formation for two sets of parameters for the star formation model (Motl et al. 2003b; 2003c). We use the Cen & Ostriker (1992) prescription to transform collapsing and rapidly cooling gas into collisionless star particles. In the star formation only sample, we assume no thermal feedback and realize the case where as many baryons are channeled into star particles as possible. This can be thought of as our cooling model with a highly selective sink available to remove cool, dense gas. In our final sample, we introduce thermal feedback to model a population of prompt supernovae. The amount of feedback has been set from numerical experiments to provide a reasonable amount of mass in star particles. The feedback is approximately 7×10^{48} *ergs* per solar mass of stars formed or about half a keV of energy per particle in the final clusters. As the degree of thermal feedback increases beyond this level there are fewer star particles formed. In the opposite extreme of no thermal feedback, we typically find that $\sim 30\%$ of baryons in our clusters are locked in star particles at the present epoch. This is incorrect but allows us to study clusters in a limiting case to gauge the importance of supernova feedback as compared to cooling and dropout (Voit et al. 2002).

In Figure 1, we show synthetic X-ray images, projected, emission-weighted temperature maps and maps of the SZE y and b parameters (eqs 2 and 3) for the most massive cluster in our sample ($M_{200} \sim 2 \times 10^{15}\ M_\odot$) evolved for each set of assumptions detailed above. Focusing on the X-ray and temperature images, we see that in the adiabatic limit the cluster is smooth in the X-ray while there is actually significant structure in the temperature map. With the addition of cooling, gas that has a short cooling time has condensed into dense, cool cores of gas. The cores significantly enhance the signature of interactions between the main cluster and infalling bodies as can be seen in the irregular patch of cool gas (cool front) extending down and to the right of the cluster center of mass. In the cooling-only limit, we find that infalling cores can survive the trip through the cluster intact and cool cores are built through the same process of hierarchical mergers that builds the cluster itself (Motl et al. 2003a). With the addition of star formation, the dense cores of gas have been "regularized", with rapidly-cooling gas being transformed into star particles. For this particular cluster, 33% of the baryons within the cluster are in star particles at the present epoch. With the addition of supernova feedback, the cluster is very similar in appearance to the star formation realization; 19% of the fluid has been transformed into star particles and they have provided $\sim 10^{62}$ *ergs* to the cluster medium throughout the simulation.

Turning to the y maps, we see that all realizations appear remarkably similar, despite the different input models. The thermal SZE measures the thermal energy content of the cluster (eq 4) which is set by the merger history that built the global cluster potential. Comparing the X-ray and y images (and the dynamic range shown in the colorbars at bottom) we see that the SZE provides a much more uniform selection function for clusters than the X-ray. For a flux-limited X-ray survey (where the X-rays sample $\propto n_e^2$), one will preferentially detect high surface brightness, cool core galaxy clusters as compared to SZE surveys that sample the density. Finally, the b maps reveal a complex pattern throughout the cluster which is qualitatively similar in all four realizations - the flow being dominated by the gravitational physics. The cluster has a net rotation with complex substructure extending beyond the cluster's virial radius into the

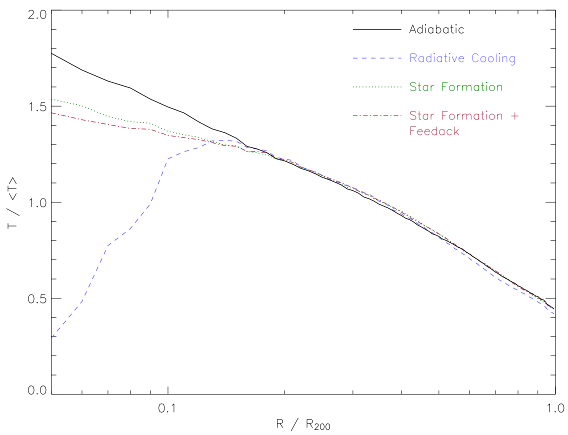

Figure 2: The average, normalized projected temperature profiles for 50 clusters in each of the four physics samples considered. The average temperature is measured within $0.5R_{200}$. All physics samples agree quite closely beyond the core region with the same, characteristic temperature profile. Also note that the two star formation samples (with and without feedback) agree well over the entire range.

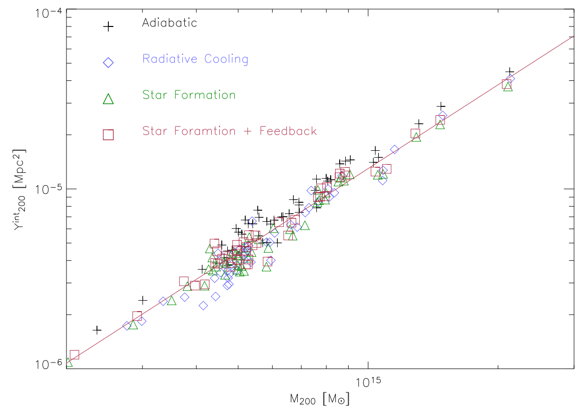

Figure 3: The scaling relation between the intrinsic Compton parameter integrated to R_{200} and M_{200} for 50 clusters in each of the four physics samples at the present epoch. The least-squares scaling relation for the Star Formation + Feedback sample is indicated by the red line. The best fit relations for the other physics samples are nearly identical.

surrounding environment. While measuring resolved flows within clusters through the kinetic SZE would be very exciting, the complex internal flows will complicate efforts to measure cluster peculiar velocities (Nagai et al. 2003; Doré et al. 2003) an effect we revisit in §3.3.

The temperature profile is a simple quantity to study given the current samples of clusters we have assembled. In Figure 2, we show the average, projected, emission-weighted temperature profile (normalized by its mean value within half the virial radius) for 50 clusters evolved in each of the physics samples. All models predict a similar decline of the temperature outside of the core of the cluster (the central 10 - 20% of R_{200} where R_{200} is the radius of a sphere containing an overdensity of 200 relative to the critical density). Within the core, the cooling model predicts a characteristic cool core profile, with the temperature falling by a factor of ~ 3. In the absence of detailed X-ray data, it would be more accurate to use the temperature profile indicated in Figure 2 than to assume that the cluster is isothermal (see Lin et al. 2003 for an application of the universal temperature profile to the measurement of the Hubble constant).

Given that the four different physical models we have considered yield similar predictions for the thermodynamic state of the gas in the majority of the cluster volume ($r > 0.2\ R_{200}$), we have cause to believe that predictions for the thermal SZE in our sample clusters are relatively independent of uncertainties in the input physics to the simulations. In Figure 3 we show the integrated, intrinsic Compton parameter (summed out to R_{200}) versus M_{200} for the same 50 clusters evolved in each of the physics models at the present epoch. The least-squares fit scaling relation is shown as the solid line for the star formation + feedback model. For the adiabatic and both star formation samples, the scaling relations are nearly identical with a slope of ~ 1.5 while the radiative cooling sample is slightly steeper with a slope of 1.6 (Motl et al. 2003d).

To reiterate, significant uncertainties in the input physics to our simulations do not impact the predicted appearance of clusters viewed through the SZE. However, clusters are dynamic, time-dependent systems and numerical simulations are crucial to study transient phenomena that are often difficult to quantify or even detect in observations. In Figure 4 we show data from a high-resolution cluster simulation (peak spatial resolution of 2 kpc with star formation and feedback included) with still frames from an animation of the y parameter and the "lightcurve" for the peak value of y from a clump that becomes part of the cluster. A major merger begins at $z \sim 0.5$ between two clusters each about $8 \times 10^{14} M_{\odot}$. The core passage from this merger is depicted in the three rightmost frames. As the cores collide (the dramatic peak in the lightcurve and the frame for $z = 0.37$), the cluster is remarkably symmetric though strongly peaked. After core passage, strong shocks expand from the center and thermalize the kinetic energy of the impact. From this merger to the present, the cluster does not interact with any other systems more massive than $\sim 10\%$ of the main cluster's mass. Mergers, which are common phenomena, greatly impact the SZE signature of a cluster for non-negligible lengths of time and can significantly bias cluster detection and measurements. Quantifying the role of cluster dynamics and calculating realistic selection functions for cluster surveys is clearly a task well suited to high-resolution, numerical simulations such as ours.

We propose a suite of numerical experiments which allow us to test the various assumptions used in observations of the SZE. These assumptions are equivalent to systematic uncertainties that limit the accuracy of the resulting data and perhaps introduce significant bias. When appropriate, we will introduce more general physical models that better describe the results from our simulations. An example of this generalization is the universal temperature profile in place of the assumption of isothermality. Specifically, we propose to subject our simulations to synthetic observations to (1) construct cosmological samples of galaxy clusters evolved with accurate and detailed input physics to quantify the importance of cluster mergers on the detection of clusters in SZE surveys and the bias mergers introduce, (2) carefully calibrate all stages in the process of transforming observables into cluster masses and (3) predict the typical kinetic SZE arising from internal cluster motions given the resolution and capabilities of various instruments

We also propose to significantly extend the state of the art in AMR cosmology simulations by including both thermal conduction and AGN feedback in our simulations. AGN outbursts in clusters, especially in the early Universe, may bias observations with the SZE through the interaction of the AGN jets with the cluster medium. Thermal conduction, on the other hand, appears capable of balancing the energy lost to X-ray radiation in a significant fraction of clusters and this energy transport mechanism should be included in realistic models.

3 Synthetic Observations

A powerful application of our simulations is to subject the full three dimensional data to mock or synthetic observations (e.g. the construction of the selection function in Lin & Mohr 2003). With known and realistic input data, key physical assumptions utilized in the reduction process can be tested and the relationship between observables and physical variables can be elucidated. We outline three specific applications of our cluster samples in the following subsections. While we ultimately will subject our complete cluster models to these numerical experiments, insight may also be gained through our existing cluster samples.

3.1 Application 1: Constructing Mass-Limited Cluster Samples

Perhaps the most important application of our work in the context of SZE surveys is to construct realistic samples of numerical clusters from mock SZE surveys (White et al. 2002; Lin & Mohr 2003). A simple example of such a survey is depicted in Figure 5 where we show a constant field of view one half a degree on a side for a region in our simulation that eventually forms a supercluster chain. The field is centered on the peak intensity of y at that redshift for the refined region and all images are prepared with the same dynamic range. This figure makes clear the significant power of SZE surveys to detect high redshift structure, many of the objects at $z = 2$ have y values comparable to those in the central regions of the $z = 0.1$ cluster. With a dimming factor of $(1+z)^4$ for X-ray observations, these high redshift structures are invisible

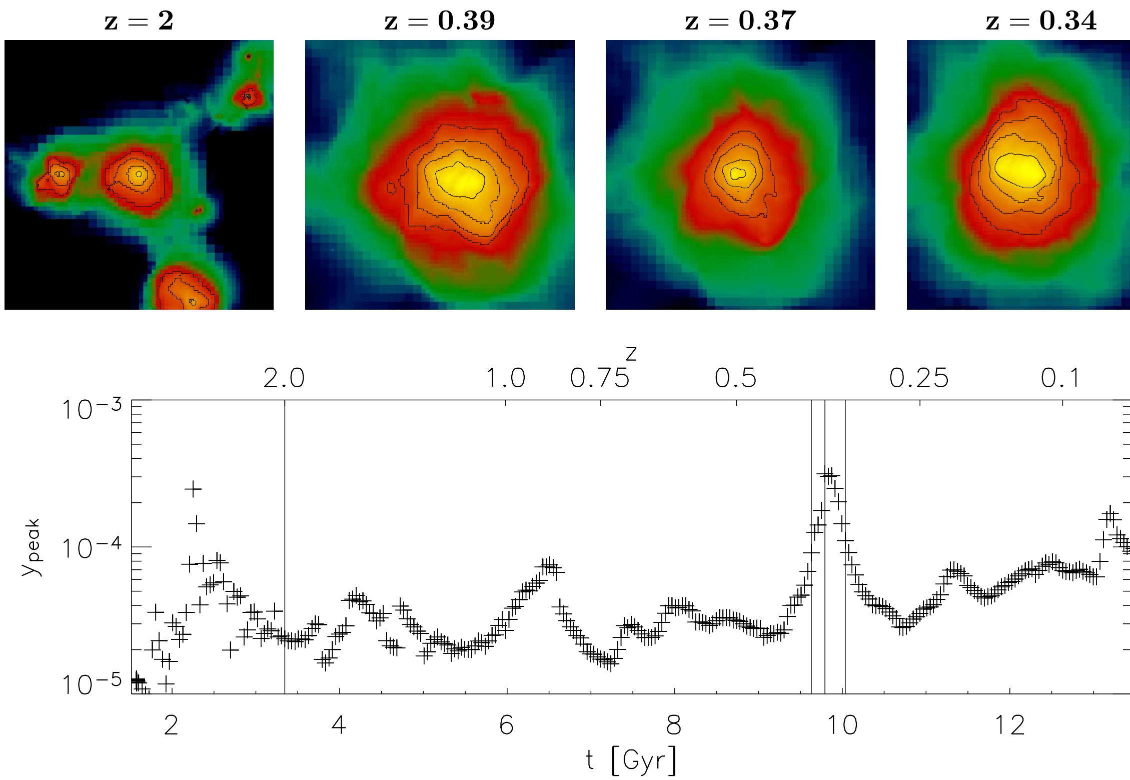

Figure 4: In the top row are still frames from an animation of the Compton y parameter from the most massive galaxy cluster in our sample ($M_{200} = 2 \times 10^{15}\ M_{\odot}$). The field of view in the images is 4 Mpc on a side at the present epoch. A major merger is depicted in the last three frames with core passage at $z = 0.37$ and images slightly before ($z = 0.39$) and after core passage ($z = 0.34$). The contours are in powers of two in y from the peak value for that frame and show that y is strongly peaked at core passage due to a shock in the core that later expands through the cluster atmosphere. The lightcurve for the peak Compton parameter is shown in the bottom plot where the vertical lines mark the times for the 4 images. The major collision at $z \sim 0.37$ boosts the value of y_{peak} by more than an order of magnitude and there are several other interactions that impact the SZE signature of the cluster throughout its evolution.

for current missions.

The results for the Y-M scaling relation shown in Figure 3 argue strongly for the invariance of SZE observables to the input physics in our models. This should not be interpreted as a statement that any particular cluster can be mapped perfectly or even without bias to a given mass. With typical free-fall velocities and masses, we can easily estimate that mergers involve energy scales up to about $10^{64} ergs$ - a significant fraction of the gravitational binding energy of a typical rich cluster. As the cluster atmosphere shock heats from these collisions it will be strongly over-pressured and have an atypically high thermal SZE signal compared to the actual mass of the cluster. This produces a merger bias (or merger boost, Randall et al. 2002) as illustrated in Figure 4. At the same time, we must consider the fact that the cluster mass function is steeply declining with increasing mass which means that mergers will boost the more abundant, lower mass systems above a given flux limit and complicate the comparison of the measured thermal SZE "luminosity" function with predictions from cosmological models.

At higher redshifts this problem will only get worse for the following two reasons. First, cluster interactions will become more common and secondly, the SZE observations will likely not have the resolution to catch and eliminate interacting systems. Nor is it clear that templates for rejecting interacting systems where mass es-

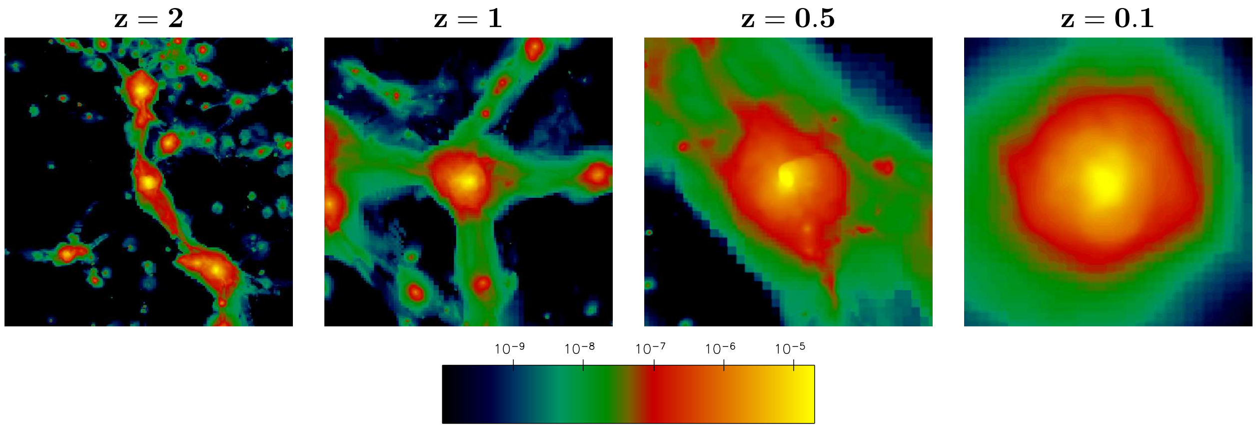

Figure 5: An example survey volume showing maps of the thermal SZE parameter y at four redshifts. The images display a constant angular region a half degree on a side for each redshift and the field of view is centered on the maximum value of y at that redshift. The dynamical range is identical for each image and therefore we would expect a significant number of detectable proto-clusters at high redshifts. The simulation evolves a rich supercluster environment from our sample volume that contains one cluster with a mass of $M_{200} = 8 \times 10^{14}\ M_{\odot}$ and two neighboring clusters more massive than $4 \times 10^{14}\ M_{\odot}$ at the present epoch. The core passage from a major merger has just occurred for the main cluster at $z = 0.5$. The simulation includes star formation with feedback and was run with a peak spatial resolution of 15.6 kpc.

timates are suspect would work, even if high-resolution SZE data were available.

To address the issue of merger bias in deep SZE surveys, we will construct a large sample of clusters such as those shown in Figure 5. The clusters can be selected by both their known mass and to a given flux detection limit. Complicating effects from CMB variation, noise, projection and resolution can be folded into the analysis as well. By comparing these two distributions we can derive an average correction function or perhaps identify a region in the mass function where an operative flux limit may be sufficiently secure. At higher masses, mergers with systems massive enough to significantly impact the cluster will become more rare and in this sense, the identification of the cluster parameters becomes more secure. Our current sample contains only a few clusters with $M > 10^{15}\ M_{\odot}$ and significant effort will be required to perform the requisite simulations and analysis.

3.2 Application 2: Measuring Cluster Masses

One of the crucial assumptions used in the interpretation of cluster observations is the appeal to hydrostatic equilibrium. Given recent advances in measurements of weak lensing sheer fields, the assumption can be tested directly by observing the same cluster in both the X-ray and by constructing weak lensing maps (e.g., Allen et al. 2001). However, it seems likely that cosmological structure, projected along the line of sight but not part of the cluster itself, should bias weak lensing masses to overestimate the true mass of the cluster (Metzler et al. 2001). In any event, the determination of cluster masses is such an important step that it is essential to check the procedure for consistency in every way possible.

While it is frequently assumed that the gas in clusters is at rest, we know from simulations that the clusters are connected to the surrounding cosmological environment through an irregular network of filaments that impose a complex and inherently three-dimensional flow field on the clusters. In Figure 6 we show a representative velocity field in the midplane of a massive cluster ($M_{200} \sim 1.5 \times 10^{15}\ M_{\odot}$). The core region has complicated flows running through it and the gas attains significant velocities (an arrow denoting a velocity of 1,500 $km\ s^{-1}$ is indicated for reference). Faced with this com-

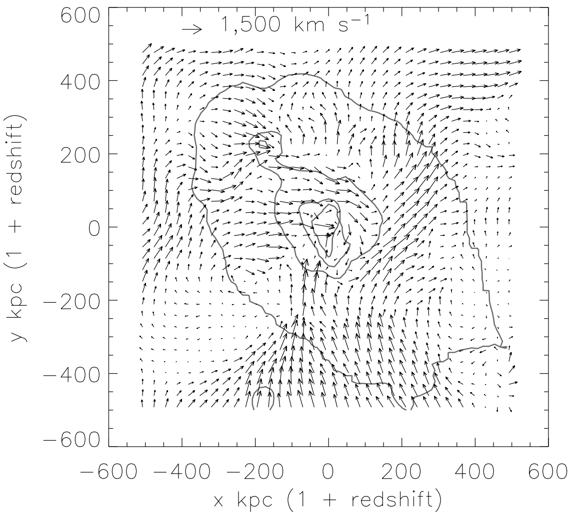

Figure 6: The velocity field for a cluster from our radiative cooling sample at $z = 0.16$ showing the central Mpc of the cluster. The X-ray surface brightness is indicated by the overlayed contours. Note the presence of bulk flows with speeds in excess of $1,000\ km\ s^{-1}$ which is comparable to the sound speed for typical temperatures.

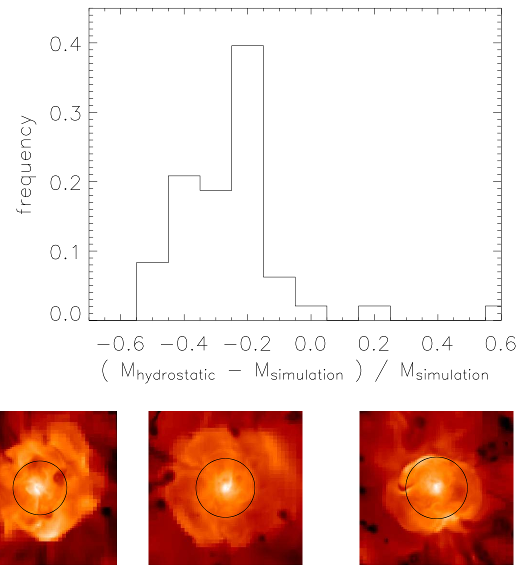

Figure 7: The frequency of relative mass errors from the assumption of hydrostatic equilibrium measured at R_{500} for 50 clusters in the adiabatic physics sample. The images at bottom are temperature maps for clusters at the far left, middle and far right end of the distribution. The images are all 5 Mpc on a side and R_{500} is indicated with a circle.

plicated flow, it is not clear that hydrostatic equilibrium will hold to high precision in real galaxy clusters. Furthermore, elementary arguments based on Euler's equations for simple flow patterns including both spherically symmetric settling and systematic rotation of the cluster demonstrate that gas motions cause an underestimate of the gravitating mass.

To illustrate our work in measuring cluster masses, we have applied the equation of hydrostatic equilibrium to the three-dimensional pressure profile from our simulated clusters in the adiabatic limit. For this example, we simply read off the estimated gravitating mass at a fiducial radius of R_{500}, assuming a spherically symmetric potential. In Figure 7, we show the distribution of relative errors in the total mass at R_{500} for 50 clusters at the present epoch. The hydrostatic mass estimate is seen to be a **biased and imprecise** estimate of the true mass. On average, one will systematically underestimate the mass by $\sim 20\%$ and errors up to 50% are possible. We also show projected, emission-weighted temperature maps for three illustrative clusters, from left to right these images correspond to the largest underestimate, a cluster in the middle of the distribution and the largest overestimate. Shock fronts and complicated temperature structure are clearly visible at R_{500} for the two extreme cases but the middle image corresponds to a fairly symmetric and relaxed looking cluster.

This example is meant to illustrate the problem and motivate further investigation of the simulations. It would be better to fully reproduce the observational process by using the projected data for the temperature and X-ray surface brightness and derive the separate, three-dimensional temperature and density profiles. However, it seems unlikely that this will reduce the errors. Rather, the results in Figure 7 would seem to represent the fundamental limit of the equation of hydrostatic equilibrium in that the only additional assumption being made is that the potential is spherically symmetric (this assumption causes a smaller error, Piffaretti et al. 2003).

Despite the simplistic approach taken here, our results stand in stark contrast to the desired properties for the hypothetical survey of Mohr et al. (2002) to measure the equation of state of dark energy. The hydrostatic mass will be a biased estimator of the true cluster mass and, on average, the systematic error will exceed 10% - even if one could reject obviously interacting systems.

3.3 Application 3: Mapping Flows within Clusters

Images of internal cluster flows - an entirely new class of observational data for clusters of galaxies - will soon be available. We have not yet been able to "see" the rich flows evidenced in Figures 1 and 6. In recent years, measurements of the internal flows have been suggested at low significance from X-ray observations with *ASCA* for Perseus (Dupke & Bregman 2001a) and Centaurus (Dupke & Bregman 2001b) through the Doppler shift of spectral features. These data have been followed by indirect observations of internal flows in Perseus with *XMM* (through the absence of resonant scattering, Churazov et al. 2003). Unfortunately, the significance and detail of the mapping has reached its practical limit for current X-ray observations, *Chandra* and *XMM* provide only a marginal improvement over *ASCA* (Dupke & Bregman 2002). However, the upcoming *ASTROE-2* mission will provide a phenomenal energy resolution of $5eV$ enabling very powerful observations of internal flows (e.g. Roettiger & Flores 2000; Sunyaev et al. 2003).

The kinetic SZE also offers the tantalizing possibility of mapping the flow field within clusters. However, the extraction of the kinetic SZE signal is very challenging as it is dominated by the thermal SZE except in a narrow range of frequencies and has a frequency dependence that is degenerate with anisotropy in the CMB itself (current measurements are reported in LaRoque et al. 2002; Benson et al. 2003). In terms of the kinetic SZE, the flows within clusters are often viewed as a contaminant as the desired quantity is the peculiar velocity of the cluster itself relative to the CMB frame (Nagai et al. 2003). Of course, using the kinetic SZE to measure internal cluster flows will be complementary to the X-ray efforts in the nearby Universe and will extend samples to much higher redshifts.

We propose to construct mock surveys with our samples of galaxy clusters to study a wide range of masses and merger histories and address concerns about the impact of internal flows on peculiar velocities. These efforts will include predictions of the projected flow patterns that should emerge from observations with *ASTROE-2*. As our simulation data will be made available through the SCA, observers can use them to model specific instruments or make comparisons to individual clusters.

4 Extension of Cluster Model Physics

As noted above, we propose to extend the physics in our cluster simulations by including both thermal conduction and also by casting AGN feedback in to the cosmological simulations through a simple, physically motivated model. While it is desirable to formulate an even more complete model for galaxy clusters, with the inclusion of magnetic fields for example, the requisite development of an AMR, MHD code is well beyond the scope of the proposed research.

In order to provide an accurate mental image of our AMR simulation technique, we now outline a typical run. For each cluster simulation, we fix two refined, nested, static grids around a sub-volume that forms a cluster of interest (identified in a previous, low-resolution run of the entire volume). The initial conditions are generated through the method of Katz et al. (1994) though the more computationally economic, multiscale framework of Bertschinger (2001) should be implemented to facilitate higher resolution simulations. These nested, static grids are embedded within the full box and finer grids are created dynamically within them to track collapsing structures. At the outset, we specify a maximum number of grid levels that limits the size of the computational problem. In a typical run, a few thousand grids exist at any one time and this scale of simulation can be run with moderate computing resources on modern supercomputers such as the new IBM p690 at the NCSA.

We wish to emphasize this point as it allows some degree of flexibility in our computational approach. We are not presently at the limit of current computing platforms. In particular, we can conduct simulations in a larger cosmological volume to reach more high mass systems or evolve larger regions with AMR to provide more representative sky samples. Most importantly, we can also push the resolution to finer scales of order 0.1 *kpc* - as will be required for simulations of AGN feedback. We note that our current *enzo* runs span a spatial dynamic range of $\sim 10^5$ but the code has been used in simulations with spatial refinement up to 10^{12} (Bryan et al. 2001).

4.1 Thermal Conduction

Interest in electronic thermal conduction in clusters of galaxies has resurfaced in the astronomical community after Narayan & Medvedev (2001) pointed out that, depending on the character of turbulent flow in clusters, disordered magnetic fields may only suppress conduction by a factor of order a few compared to the classical Spitzer value. While at the recent Charlottesville meeting, "The Riddle of Cooling Flows in Galaxies and Clusters of Galaxies", thermal conduction was somewhat disparaged as a relevant mechanism in clusters (cf Soker 2003), we feel that the case for conduction has become stronger since the original work by Narayan and Medvedev. On the theoretical front, numerical simulations of MHD turbulence by Chandran & Maron (2003) and Cho et al. (2003) have supported their basic prediction. On the observational front, recent work by Medvedev et al. (2003), Zakamska & Narayan (2003) and Voigt & Fabian (2003) have found that many clusters are consistent with thermal conduction balancing the energy lost to radiation for suppression factors of order a few.

The impact of thermal conduction on the temperature profiles shown in Figure 2 is of obvious theoretical interest. In order to address this question with our simulations we will develop a new module for our AMR code to solve the gas energy equation including the effects of thermal conduction. The module will implement three options for choosing thermal conductivities: (1) constant, (2) Spitzer (classical) and (3) saturated (e.g., Cowie & McKee 1977). For options 2 and 3, a reduction factor (≤ 1) can be specified to take into account the reduction of electron mean free paths due to tangled magnetic fields (Malyshkin & Kulsrud 2001). We have already developed an optimal spatial differencing scheme for the conduction operator and work is currently underway to implement a stable and accurate treatment of the competing heat fluxes into and out of a fluid cell in a timestep.

With this addition to our code we will be able to measure the impact of thermal conduction on the properties of clusters evolved in a realistic cosmological context. While thermal conduction is likely not going to strongly modify the SZE appearance of clusters in the nearby Universe, it will likely mold the structures that merge to form clusters at high redshifts (Fabian et al. 2002). Since the conduction coefficient scales as $T^{5/2}$, conduction may also produce interesting differences between high and low mass clusters.

4.2 AGN Feedback

AGN are seen to have a significant impact in the cores of many nearby galaxy clusters. An example image from Abell 2052 is shown in Figure 8. For M87 (Owen et al. 2000) and the Perseus cluster (Fabian et al. 2003), there is also evidence that AGN erupt cyclically. From a theoretical point of view, AGN are sufficiently energetic to significantly perturb clusters (Ensslin et al. 1998; Wu et al. 2000), especially in the high redshift universe when AGN were brighter and the confining cluster potential was shallower. In terms of the SZE, the mechanical action of AGN jets on the ICM will over-pressure portions of the cluster atmosphere and result in a cluster with too large a thermal SZE signature for the mass of the cluster - a potentially significant source of bias. Furthermore, the preheating in semi-analytic (e.g. McCarthy et al. 2003) and hydrodynamic simulations (daSilva et al. 2003) ultimately arises from AGN and a more accurate approach is to model this directly.

Omma et al. (2003) recently presented a novel method for incorporating an AGN jet into AMR

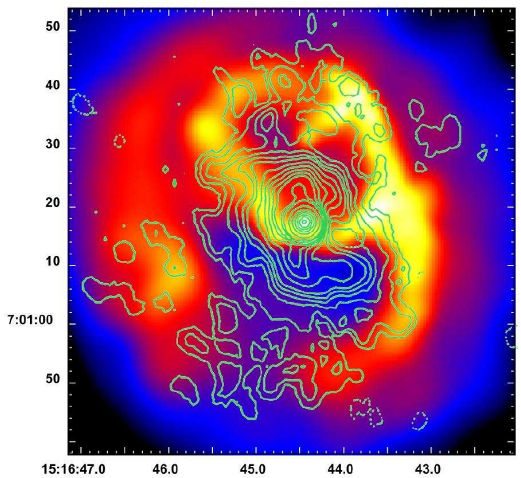

Figure 8: Adaptively smoothed Chandra ACIS-S3 image of the central region of Abell 2052 from Blanton et al. (2003) with radio contours (Burns 1990) superposed. The radio source appears to have swept out "bubbles" in the X-ray emitting gas, creating bright shells of compressed X-ray gas surrounding the holes.

simulations. They launch jets from a small region at the center of an initially static and spherical cluster atmosphere. *We propose to extend their work by merging their jet model into our cosmological simulations.* We emphasize for clarity that we will not attempt to solve the AGN feeding problem or track the mergers of super-massive black holes as proto-galactic and galactic halos merge. Rather, we are concerned with developing a phenomenological model that can produce a plausible amount of energy input with a realistic frequency of outburst events.

The key point to our approach is the coupling of Omma's jet algorithm to parameters available in our cosmological simulations. We propose to couple the initial conditions for the jet to the local star formation rate in the star particle halos that roughly approximate galaxies. There will then be one input parameter that maps the strength of a "starburst" to the AGN fueling rate. With this approach, we will naturally account for the decline in AGN luminosity as the global star formation rate declines through the simulations. In addition, the model is sufficiently complex to allow for multiple outbursts or feedback cycles as the cluster gas cools, forms stars and "feeds" the AGN which heats the cluster. More complicated models are easily envisaged. For example, the halo mass can serve as a surrogate for $M_\bullet$ which could then modify the jet according to the expected accretion environment (Heinz & Sunyaev 2003).

The original orientation of the jets for a given stellar halo will be random and over time, the instantaneous orientation will be computed as a weighted sum of previous orientations with small perturbations. We will ascribe the instantaneous launch region to be at the center of mass of the stellar halo at that point in the simulation. To incorporate the work of Omma et al., we must perform simulations with a peak spatial resolution of approximately 0.1 kpc. As noted above, this resolution is within the reach of our simulation tool running on current platforms.

While this approach will obviously require significant development and testing it will allow us the unique opportunity of tracing jet dynamics in a realistic cluster environment where the full complexity of the cluster medium is naturally accounted for. Furthermore, this work will allow us to gauge the importance of AGN feedback on clusters in a similar manner to our previous work with cooling, star formation and supernova feedback. These simulations will be, to our knowledge, the first to directly model AGN jets in galaxy clusters that evolve in a cosmological setting.

5 Education and Outreach

We propose several mechanisms to broaden the reach of the work detailed here to the astronomical community and to involve and inspire future scientists as well. First, as we have done previously, we will make all data from our proposed simulations available to the astronomical and broader scientific community through our Simulated Cluster Archive. In addition to providing an interface to the data, the SCA contains many attractive graphics that illustrate our simulations (see also http://casa.colorado.edu/∼motl). We will continue to produce illustrations such as these as a service to the community and in particular to educators. Complex physics such as hydrodynamics in a cosmological context can be easily understood by undergraduate and even high school students through a high-quality and carefully prepared graphical representation.

We will also recruit an undergraduate astrophysics major at the University of Colorado (or perhaps two students, non-concurrently) to participate in the work we propose here. Our simulations use cutting-edge numerical techniques and there are a myriad of introductory, small-scale projects to introduce a promising student to sophisticated research that likely will be of considerable value in their upcoming career in science. The undergraduate researchers will focus on a specific research project and follow it through every step including literature research, formulation of the measurement, analysis and finally preparing the project for presentation in an appropriate forum (a poster presentation at CU or at an AAS meeting and ultimately in a peer-reviewed publication). Experiencing the complete life cycle of a research project is, we believe, one of the most valuable experiences available to a young scientist.

Finally, we propose to incorporate our research efforts into the highly successful Pre-Collegiate Development Program (PCDP) through the University of Colorado. PCDP exists to facilitate the transition to college for middle and high school students who are, statistically speaking, currently under-represented in higher education whether they would represent the first generation to attend college or face difficulties such as growing up in a single parent household. In the 2003-04 academic year over 2,000 students participated in the program (85% of participants are students of color) and 96% of students who graduate from the PCDP go on to attend college.

While computational astrophysics is an advanced subject a certain kernel of the experience is easily digestible, especially when the story can be told with the aid of powerful graphics and animations. We propose to partner with an area high school participating in the PCDP and provide our services to teach aspects of contemporary astronomy and cosmology on a regular (monthly) basis as a supplementary activity. In particular we will focus on aspects of the research described here. In reality, however, any topic from science can be used to spark interest - the story is more in the telling than in the facts themselves. However, simulated realities have a certain cache with students and it is hoped that it will inspire them to further engage in science and computer technology. We will also take full advantage of the facilities available in the Denver-Boulder metropolitan area including the Fiske planetarium and Sommers-Bausch observatory at the University of Colorado as well as the new Space Odyssey exhibit at the Denver Museum of Nature and Science.

6 Summary and Work Plan

In closing, we have outlined an extensive research program that we believe is crucial to bringing the full power of SZE surveys to fruition. To realize the potential of the data, there must be careful control of the systematics introduced by modeling to measure values of interest. Direct numerical simulations are a critical tool in studying and eventually controlling these systematic biases and errors of interpretation by processing the simulation data through synthetic observations.

Our simulations will incorporate increasingly complex input physics to describe the clusters including radiative cooling, star formation, supernova feedback, electronic conduction and feedback from AGN. Our simulation tool has been developed through a long-term collaboration with Mike Norman and Greg Bryan and we will continue to work with them on the research efforts outlined in this proposal. Jason Glenn, a member of the Bolocam team. is also at the University of Colorado and we will work with him to apply our simulations to the interpretation of Bolocam observations.